



RESEARCH

Open Access



# Optimized GMP-grade production of non-viral Sleeping Beauty-generated CARCIK cells for enhanced fitness and clinical scalability

Ilaria Pisani<sup>1†</sup>, Giusi Melita<sup>1†</sup>, Patricia Borges de Souza<sup>2</sup>, Stefania Galimberti<sup>3</sup>, Angela Maria Savino<sup>4</sup>, Jolanda Sarno<sup>4</sup>, Beatrice Landoni<sup>1</sup>, Stefano Crippa<sup>1</sup>, Elisa Gotti<sup>5</sup>, Carolina Cuofano<sup>5</sup>, Olga Pedrini<sup>5</sup>, Chiara Capelli<sup>5</sup>, Giada Matera<sup>6</sup>, Daniela Belotti<sup>6</sup>, Stefania Cesana<sup>6</sup>, Benedetta Cabiati<sup>6</sup>, Michele Quaroni<sup>6</sup>, Valentina Colombo<sup>6</sup>, Massimiliano Mazza<sup>2</sup>, Barbara Vergani<sup>4</sup>, Anna Gaimari<sup>2</sup>, Fabio Nicolini<sup>2</sup>, Marcella Tazzari<sup>2</sup>, Martine Bocchini<sup>2</sup>, Marta Serafini<sup>1,4</sup>, Alessandro Rambaldi<sup>7,8</sup>, Benedetta Rambaldi<sup>8</sup>, Giuseppe Dastoli<sup>1</sup>, Andrea Biondi<sup>1</sup>, Giuseppe Gaipa<sup>1\*</sup> , Martino Introna<sup>5</sup>, Josée Golay<sup>5</sup> and Sarah Tettamanti<sup>1</sup> 

## Abstract

**Background** Strict adherence to GMP guidelines and regulatory compliance is crucial when transitioning from research to clinical-grade production of ATMPs like CAR T cells. The success of CAR T cell therapy in treating hematological malignancies highlights the need for closed or automated systems to ensure quality and efficacy. Recent evidence also suggests that ex vivo culture conditions can significantly impact CAR T cell functionality.

**Methods** We present our optimized methodology for expanding Sleeping Beauty transposon-engineered Chimeric Antigen Receptor-Cytokine-Induced Killer (CARCIK) cells using G-Rex devices and evaluate its impact on CARCIK cell phenotype and T cell fitness.

**Results** Building on our previously validated protocol, we introduced key simplifications to optimize the CARCIK differentiation process. Delaying the nucleofection step eliminated the need for feeder cells while maintaining efficient CAR expression and high cell viability. Transitioning from T-flasks to G-Rex bioreactors reduced operator hands-on time from 21 to 28 days to 14–17 days and resulted in a less differentiated CARCIK cell product. Metabolic and transcriptional analyses showed that the novel protocol improves CARCIK cell fitness and *in vivo* efficacy against B-cell lymphoma. The novel method was validated in Good Manufacturing Practices (GMP) conditions at our two Cell Factories and yielded enough numbers of CARCIK-CD19 cells for clinical use.

**Conclusions** Optimizing non-viral CARCIK cell production using G-Rex bioreactors and refined timing adjustments has streamlined the workflow, enhanced cell fitness, and resulted in a highly effective therapeutic product with demonstrated *in vivo* efficacy in mice. These improvements reduced manipulation and contamination risks, while

<sup>†</sup>Ilaria Pisani and Giusi Melita equally share the first author position to this work.

\*Correspondence:  
Giuseppe Gaipa  
giuseppe.gaipa@ircs-sangerardo.it

Full list of author information is available at the end of the article



© The Author(s) 2025. **Open Access** This article is licensed under a Creative Commons Attribution-NonCommercial-NoDerivatives 4.0 International License, which permits any non-commercial use, sharing, distribution and reproduction in any medium or format, as long as you give appropriate credit to the original author(s) and the source, provide a link to the Creative Commons licence, and indicate if you modified the licensed material. You do not have permission under this licence to share adapted material derived from this article or parts of it. The images or other third party material in this article are included in the article's Creative Commons licence, unless indicated otherwise in a credit line to the material. If material is not included in the article's Creative Commons licence and your intended use is not permitted by statutory regulation or exceeds the permitted use, you will need to obtain permission directly from the copyright holder. To view a copy of this licence, visit <http://creativecommons.org/licenses/by-nc-nd/4.0/>.

optimizing logistics and space efficiency, facilitating allogeneic CARCIK generation for a current phase I/II clinical trial (NCT05869279) in patients with R/R CD19+ non-Hodgkin Lymphoma (B-cell NHL) and Chronic Lymphocytic Leukemia (CLL), confirming the approach's scalability and clinical potential.

**Keywords** Good manufacturing practices (GMP), CAR T cells, Hematological malignancies, Sleeping beauty transposon, Workflow optimization, T cell fitness

## Background

Chimeric antigen receptor (CAR) T cell therapy has demonstrated remarkable efficacy in treating B-cell malignancies. The most prevalent method for genetically modifying T cells to express CAR transgenes relies on viral vectors, which entails notable drawbacks, including high costs, safety concerns, and production challenges. Non-viral methods, such as transposon/transposase systems, present a safer and more cost-effective platform and offer promising alternatives bypassing some of the challenges typically associated with viral vectors [1].

In our prior work, we developed a successful non-viral engineering platform using the Sleeping Beauty (SB) transposon system for CAR T cells targeting CD19 [2], CD33 [3], CD123 [4], and BAFFR [5]. In particular, the transposon-based CAR-CD19 modified Cytokine-Induced Killer (CARCIK-CD19) cell product has been clinically validated in GMP and used to treat adult and pediatric patients with B-Acute Lymphoblastic Leukemia (ALL) relapsed after allogeneic hematopoietic stem cell transplantation (allo-HSCT) (NCT03389035). CARCIK-CD19 cells were generated from the original donor mononuclear cells, proving feasibility and safety [6]. A subsequent trial is ongoing to test the impact of a second CARCIK-CD19 infusion in relapsed/refractory B-cell precursor ALL, guided by the initial response after the first infusion (NCT05252403).

The clinical insights accumulated so far from CAR T cell therapies highlighted the critical role of ex vivo CAR T cell expansion, including the duration of the production process, the selection of plastics and devices for cell growth, and the use of various media and supplementary cytokines for the feasibility and efficacy of the procedure [7]. All these factors collectively significantly influence CAR T cell function, ultimately impacting the overall potency of these cells upon their application in clinical settings. With the goal of streamlining the entire CARCIK manufacturing procedure and to further optimize our CARCIK-CD19 cell product, we leveraged our established success in producing unmodified CIK cells with the G-Rex bioreactor [8], integrating into the process the non-viral genetic manipulation with the SB system.

G-Rex devices are closed-culture vessels featuring a gas-permeable silicone membrane at the base. This design supports efficient gas exchange and nutrient delivery while maintaining a stable cell culture environment. By allowing for the addition of a large medium volume

at the start of the process, these devices reduce the need for frequent handling and minimize contamination risks, streamlining workflows and supporting robust cell growth [9]. The G-Rex devices have proven instrumental in cell expansion of various T cell types, including antigen-specific T cells, tumor-infiltrating lymphocytes (TILs) [10], regulatory T cells (Tregs) [11],  $\gamma/\delta$  T cells [12], CAR T cells [13], and CIK [8], for both research and clinical purposes.

We present here the results of the optimization and process simplification, *in vitro* and *in vivo* characterization, and GMP validation of CARCIK-CD19 cell expansion in G-Rex devices. When compared with CARCIK-CD19 cells expanded in T-flask, G-Rex cultured cells demonstrated: (I) a higher memory profile; (II) a metabolic profiling more skewed towards mitochondrial respiration and (III) transcriptional profiling suggesting an optimized fitness profile. These differences were reflected in a potent *in vivo* efficacy, enabling a reduction in the necessary cell dose to achieve control over tumor growth in mice. The new production process is currently exploited to generate allogeneic CARCIK-CD19 cells in a phase I/II study to treat adult and pediatric patients with R/R mature CD19+ B-NHL and CLL (NCT05869279).

## Materials and methods

### Manufacturing

Human peripheral blood mononuclear cells (PBMCs), obtained from healthy subjects upon informed consent, were isolated on density gradient using Ficoll-Hypaque (Pharmacia LKB, Uppsala, Sweden) and were plated in standard tissue culture T-flasks (Thermo Fisher Scientific, Waltham, MA; or Becton Dickinson, Franklin Lakes, NJ) at  $3 \times 10^6$ /mL in Advanced RPMI-1640 Medium (Gibco, Thermo Fisher Scientific) supplemented with 10% heat-inactivated fetal bovine serum (FBS, HYCLONE), 2mM L-glutamine, 25 IU/ml of penicillin and 25 mg/ml of streptomycin (Lonza, Basel, Switzerland). MNCs were supplemented on day 0 with IFN- $\gamma$  (1000 IU/mL; Boehringer Ingelheim) and on day 1 with 50 ng/mL anti-CD3 (OKT3; Takara) and 300 IU/mL recombinant human (rh)IL-2 (Novartis). For cells electroporated on Day 0, the established protocol was followed [2]. In the new, simplified process, cells were electroporated on Day 2 with GMP-grade CD19.CAR/pT4MNDU3 and pCMV-SB100X plasmids (manufactured by ALDEV-RON). Briefly, PBMCs were electroporated using the

4D-Nucleofector System (Lonza) with the P3 Primary Cell 4D-Nucleofector Kit (Lonza) in the presence of a pT4 SB vector expressing the FMC63-derived CD19-specific scFv fused to a CD28 transmembrane domain and the CD28.OX40.CD3 $\zeta$  signaling endodomain under the control of the synthetic MNDU3 [14] promoter and flanked by pT inverted repeats (IR)/direct repeats (DR) sequences [15] and the pCMV vector encoding the transposase SB100X gene [16]. The CARCIK expansions were carried out in the G-REX bioreactor (ScaleReady™), and were compared in parallel with the standard culture method employing the T-flasks. Briefly, for the G-REX culture, CARCIK cells were transferred in the G-Rex from the 6-well plate after one week and were kept in the bioreactor for 10 days, with the sole addition of IL-2 every 3 days. For the T-flasks culture, CARCIK cells were transferred in the T-flask by day 4, and thereafter counted and split every 3 days with the addition of fresh medium and IL-2 until day 21.

#### Cell lines

DAUDI, REH and THP-1 cell lines were originally obtained from the American Type Culture Collection (ATCC). The DAUDI (human Burkitt's Lymphoma) and THP-1 (Acute Myeloid Leukemia, AML) cell lines were maintained in RPMI 1640 medium (Sigma Aldrich, St. Louis, Missouri, USA) supplemented with 10% heat-inactivated fetal bovine serum (FBS), 2mM L-glutamine, 25 IU/ml of penicillin and 25 mg/ml of streptomycin (Lonza, Basel, Switzerland) at a concentration of around  $0.3 \times 10^6$  cells/ml. The human cell line REH (pre-B-ALL, CD19+) was maintained in RPMI-1640 (Euroclone, Wetherby, West Yorkshire, UK) supplemented with 10% fetal bovine serum (FBS; Euroclone), 2 mM L-glutamine (Euroclone) and 110  $\mu$ M gentamycin (PHT Pharma, Milano, Italy).

#### Flow cytometry

Flow cytometry was used to investigate CARCIK-CD19 phenotype by quantification of CD3 (clone: SK7, Biolegend), CD4 (clone: RPA-T4, Biolegend), CD8 (clone: SK1, Biolegend), CD56 (clone: NCAM16.2, BD bioscience). CAR-CD19<sup>+</sup> cells were detected after incubation with human recombinant CD19his (rhCD19his, Thermo Fisher Scientific) followed by anti-His (Miltenyi Biotec) antibodies. In addition, CD62L (clone: DREG56, BD bioscience) and CD45RO (clone: UCHL1, BD bioscience) were used to characterize the memory profile. Human grafts in mice were assessed using anti-mouse CD45 (clone: 30-F11, eBioscience), anti-human CD45 (clone: HI30, ThermoFisher), CD19 (clone: J3-119, Beckman Coulter) and CD3 (clone: SK7, Biolegend). All the samples were acquired on a FACS-Canto and data were analysed using BD FACSDiva Software.

#### Cytotoxicity assay

To measure cytotoxic potential, CARCIK-CD19 cells were co-cultured for 4 h with the CD19<sup>+</sup> REH cell line at an effector-target (E: T) ratio of 5:1. Before incubation, target cells were stained with CFSE (Carboxyfluorescein succinimidyl ester) and then after the incubation period cells were labelled with annexin V and Necrosis Detection Reagent (NDR) using a GFP-certified apoptosis/necrosis detection kit (ENZO lifesciences) and the fluorescence was analysed on a FACS Canto- Flow Cytometer (BD). The proportion of killed cells was determined by measuring the percentage of total target (CFSE<sup>+</sup>) dead cells (annexin<sup>+</sup>NDR<sup>-</sup> early apoptotic cells, annexin<sup>+</sup>NDR<sup>+</sup> late apoptotic cells and annexin<sup>-</sup>NDR<sup>+</sup> necrotic cells) and applying the following calculation:

$$\% \text{ Cytotoxicity} = \frac{\% \text{ of CFSE}^+ \text{ dead cells in coculture} - \% \text{ spontaneous death of CFSE}^+ \text{ cells}}{100 - \% \text{ spontaneous death of CFSE}^+ \text{ cells}} \times 100$$

#### Vector copy number detection

DNA from CARCIK-CD19 cells was extracted using the QIAamp DNA Mini Kit (QIAGEN). Real-TIME qPCR was performed on 100ng of DNA extracted from  $5 \times 10^6$  CARCIK cells using QIAamp DNA Mini Kit (QIAGEN) using the TaqMan Gene Expression Master Mix (Applied Biosystems) and TaqMan qPCR (RT-PCR System QuantStudio 3, Applied Biosystems) to compare the gene expression of hRNaseP (as housekeeping) and VCN. The precise method and primers are described in our previous publications [2, 6].

#### Detection of SB100X transposase enzyme

RNA from CARCIK-CD19 cells was extracted using the QIAamp RNA mini kit and retrotranscribed with SuperScript IV VILO master mix. qPCR amplification of homologous regions within SB100X transcripts was performed using TaqMan gene expression master mix and FastStart universal probe master. Specific primers and a UPL probe were used. Copy number quantification was based on a seven-point standard curve of plasmid DNA dilutions. Data were normalized using the  $\beta$ -glucuronidase gene (GUS) and analyzed with the delta-delta CT (ddCT) method, as previously described [3].

#### Seahorse assay

$1 \times 10^6$  T cells were resuspended in 5 mM glucose and 2 mM glutamine RPMI XF medium and plated in a previously Poly-D-lysine hydrobromide (Sigma-Aldrich) coated XF96/XFpro microplates. After a centrifugation at 200 g for 1 min (no brake) and incubation for 1 h at 37 °C in a non-CO<sub>2</sub> environment the assay was launched on the instrument using Seahorse XF T cell persistence template. First, the basal OCR (oxygen consumption

rate) and ECAR (extracellular acidification rate) condition were measured using Seahorse XF96 Extracellular Flux Array kit and Seahorse XF T cell metabolic profiling kit (both from Agilent, Madison, WI), then the samples were read. Final data were exported into an Excel (v.2311) using Agilent software and converted into graphs.

#### Nanostring immune exhaustion panel characterization

RNA from CARCIK-CD19 cells was extracted using the QIAamp RNA mini kit and stored at -80 °C. RNA samples were thawed and RNA integrity and quantity were assessed using the 2100 Bioanalyzer (Agilent) according to manufacturer's instructions and subsequently subjected to gene expression analysis using the Nanostring nCounter® platform. The Immune Exhaustion Panel (ref. XT-H-EXHAUST-12, Nanostring) was employed to assay specific gene signatures involved in immune cell function. For each sample, 50 ng of total RNA was hybridized at 65 °C for 22 h with a combination of standard probes, according to the manufacturer's guidelines. The samples were then loaded onto the Nanostring Automated nCounter® Prep Station equipped with the FLEX system for cartridge preparation and further processing. Raw expression data were analyzed using nSolver Analysis Software 4.0 (Nanostring) and normalized by housekeeping genes and positive controls. To evaluate the impact of the type of culture (flask or G-Rex) on key biological pathways we enabled pathway scoring analysis, which allows for the assessment of pathway activation scores based on gene expression data. Differential expression was assessed considering culture as the predictor, with no confounding variables included. To control for the false discovery rate, we used the Benjamini-Yekutieli procedure. Gene set analysis was also performed to assess the enrichment of specific gene sets across conditions. Data visualization and results were generated by nSolver Analysis Software 4.0 (Nanostring) or python with matplotlib and seaborn modules.

#### *in vivo* studies

The study was approved by the Italian Ministry of Health. Procedures involving animals were conformed with protocols approved by the Milano-Bicocca University in compliance with national and international law and policies. All *in vivo* experiments were conducted at the University of Milano-Bicocca. Six- to eight-week-old male NSG mice (NOD.Cg-PrkdcscidIl2rgtm1Wjl/SzJ) (Charles River Laboratories) were sub-lethally irradiated (200 cGy) before the infusion of tumor cells. Four hours later  $2 \times 10^5$  DAUDI cells (both wild type and Luciferase-modified ones) were i.v. infused. Depending on the experiment, different doses of CARCIK-CD19 cells were i.v. injected at day 2 after DAUDI IV.

When DAUDI cells were used, 50 µl of Peripheral Blood (PB) samples were taken from the mice every 10 days and stained with hCD45, mCD45, hCD3 and hCD19, to evaluate the presence of tumor and/or CARCIK-CD19 cells as compared to the control group of untreated mice (DAUDI only). When Daudi-FFLuc + were used, bioluminescence imaging was performed using an IVIS Lumina III imaging system (PerkinElmer, USA). Whole-body imaging was performed 12 min after subcutaneous injection with 150 mg/kg firefly D-luciferin (PerkinElmer, USA) in isoflurane-anesthetized mice. Image processing was carried out with a background subtraction using Living Image software (PerkinElmer, USA) and expressed as photons/s (Total flux). Once mice were euthanized, spleens were analyzed by flow cytometry and RNAscope to assess the presence of CARCIK-CD19 cells as well as tumor.

#### Histological analyses on FFPE mouse specimens

Formalin-fixed, paraffin-embedded (FFPE) tissue specimens were sectioned at 5 µm thickness. A custom 12-zy probe was designed to target the scFv domain of CARCIK mRNA (3596–4397 bp of CAR-cassette, covering the Leader sequence, VL-linker-VH), and an inventoried zy probe targeted tumor cell at the hs-CD19-C2 domain. Both probes were validated *in silico* for sensitivity and specificity. Samples were processed following the RNAscope (ACDBio) protocol. Duplex RNAscope® probes for CAR-CIK (Channel 1, green) and CD19 (Channel 2, red) were hybridized at 40 °C for 2 h using the HyBEZ™ Hybridization System II. Signal amplification and detection utilized the RNAscope® Kit 2.5 HD Duplex Detection Kit (Cat. 322500), followed by red and green chromogenic revelation and Gill's hematoxylin nuclear counterstaining. Slides were mounted using Vectamount® medium. Additionally, FFPE mouse slides underwent CD3 (Clone 2G6, Roche) staining on a Ventana Benchmark ULTRA system with the Optiview DAB Detection Kit and UltraView Universal Alkaline Phosphatase Red Detection Kit. Hematoxylin II counterstaining was performed for 16 min after immunostaining. High-resolution whole-slide images (40x magnification) were acquired using the Aperio CS2 slide scanner (Leica Biosystems).

#### RNAscope positive and negative controls

To ensure reliable RNAscope assay validation mouse samples and HeLa cells Control Slides (ACDBio, Cat. 310046) were stained using the Duplex Positive Control probe Hs PPIB-C1 / Polr2A-C2 (ACDBio, Cat. 321641) and the Duplex Negative Control probe DapB-C1 / DapB-C2 (ACDBio, Cat. 320751).

### Statistical analysis

Categorical variables are described by counts and percentages, and quantitative characteristics are expressed as median (I-III quartile) or mean (standard deviation, SD), as appropriate. Wilcoxon signed-rank test or the Turkey's test were used for comparing quantitative variables between two paired or unpaired samples, respectively. Kaplan-Meier method was applied to estimate survival curves, while the log-rank test for comparisons. *P*-values were adjusted for multiple testing using the Benjamini-Hochberg method. Analyses were performed using R 4.2.1 (R Foundation for Statistical Computing, Vienna, Austria) and GraphPad Prism (La Jolla, CA, USA) softwares. *P*-values are denoted with asterisks as follows: *p*-value > 0.05, not significant (ns); *p*-value < 0.05; \*, *p*-value < 0.01; \*\*, *p*-value < 0.001; \*\*\*, *p*-value < 0.0001.

### Results

#### Streamlining of non-viral CARCIK differentiation: validation of DNA SB plasmid dose and feeder-free nucleofection

To mitigate post-nucleofection toxicity, primarily associated with the quantity of exogenous DNA, and obtain the maximum CARCIK cell yield, we conducted titration assays using the pT4 transposon, carrying a third-generation CD19.CAR, and SB100X transposase plasmids. Additionally, to streamline the production process, CARCIK-CD19 cells were transferred to the G-Rex bioreactor on day 7 and compared with the standard T-flask (Flask)-based culture method. The G-Rex system successfully shortened the culture period to 14–17 days, compared to the 21–28 days required with Flasks. To determine the optimal plasmids' concentration, PBMCs were electroporated with 10 µg and 7.5 µg of pT4 transposon, coupled to 0.5–1 µg of SB100X transposase, respectively. Our findings identified the 7.5 + 1 titration point as optimal, in terms of cell counts (Fig. 1A) and elevated CAR expression (Fig. 11B), while maintaining the typical CIK phenotype (Fig. 1C).

As an additional implementation to the standard protocol [2, 17], we observed that we could remove the need for gamma-irradiated PBMCs at day 0 by postponing the nucleofection step. For these experiments, we employed optimized doses of pT4 and SB100X, alongside the parallel use of the G-Rex system or Flasks. Nucleofection performed on day 1, precisely 24 h after the addition of IFN-γ, failed to yield satisfactory CAR expression and resulted in diminished cell numbers (data not shown). In contrast, day 2 transfection (Day 2), carried out 24 h after stimulation with anti-CD3 OKT3 and IL-2, emerged as the earliest differentiation point that provided cell numbers (Fig. 1D), CAR percentage (Fig. 1E), a CIK phenotype (CD3<sup>+</sup>CD56<sup>+</sup> cells, Fig. 1F) and CD8/CD4 ratio (Fig. 1G),

closely resembling, if not exceeding, those achieved using the standard protocol. Both Flask- and G-Rex-expanded CARCIK-CD19 cells displayed potent in vitro killing ability against the CD19<sup>+</sup> REH cell line (Fig. 1H). Vector Copy Number (VCN) and SB100X transposase detection confirmed the expected safety of the CARCIK-CD19 produced with the optimized process, in agreement with the current clinical protocol requirements (VCN: < 5copies/cell; SB100X: < 20 copies/10000 GUS) (Fig. 1I). Overall, the improvements made to the standard production process (Protocol 1) allowed for a reduction in SB plasmid quantities, simplification of cell culture procedures, and a decrease in culture time, while still achieving suitable numbers of CARCIK-CD19 cells for clinical use (Protocol 2) (Fig. 1L).

#### Expansion in G-Rex bioreactors produces less differentiated CARCIK cells

The consistency and reproducibility of the new production process were validated by performing multiple CARCIK-CD19 expansions (Fig. 2) and successfully extending it to other CARs, such as CD33CAR (Supplemental Fig. 1A-C). Since the differentiation status of infused T cells is increasingly recognized as a critical parameter for enhanced persistence and anti-tumor immunity [18, 19], we conducted a comparison of the memory phenotype between GMP-grade CARCIK cells generated using the standard protocol cultured in Flasks (GMP runs, Protocol 1, *n* = 28) versus those generated using the optimized procedure and expanded in G-Rex bioreactors (G-Rex, Protocol 2, *n* = 10). Interestingly, CARCIK cells produced applying Protocol 2 showed a significant enrichment in central memory (CM) populations and a reduction in terminally differentiated EMRA populations compared to GMP runs using Protocol 1 (Fig. 2B). Notably, the transition from Flasks to G-Rex bioreactors contributed to the development of a less differentiated memory phenotype in CARCIK cells, consistently observed within individual donors using the same PBMC source and following Protocol 2 (Fig. 2C) and by looking at the memory dynamic evolution over time in culture (Supplemental 1D). The overall change in memory profile was also functionally validated by real-time metabolic profiling using the Seahorse Analyzer. Indeed, G-Rex-expanded CARCIK cells demonstrated a reduction in the extracellular acidification rate (ECAR) and an increase in respiration parameters, including basal and spare capacity, as measured by the oxygen consumption rate (OCR). Additionally, these cells exhibited elevated mitochondrial ATP production (Fig. 2D-E). These metabolic characteristics are typically associated with naïve and central memory T cells [20, 21].



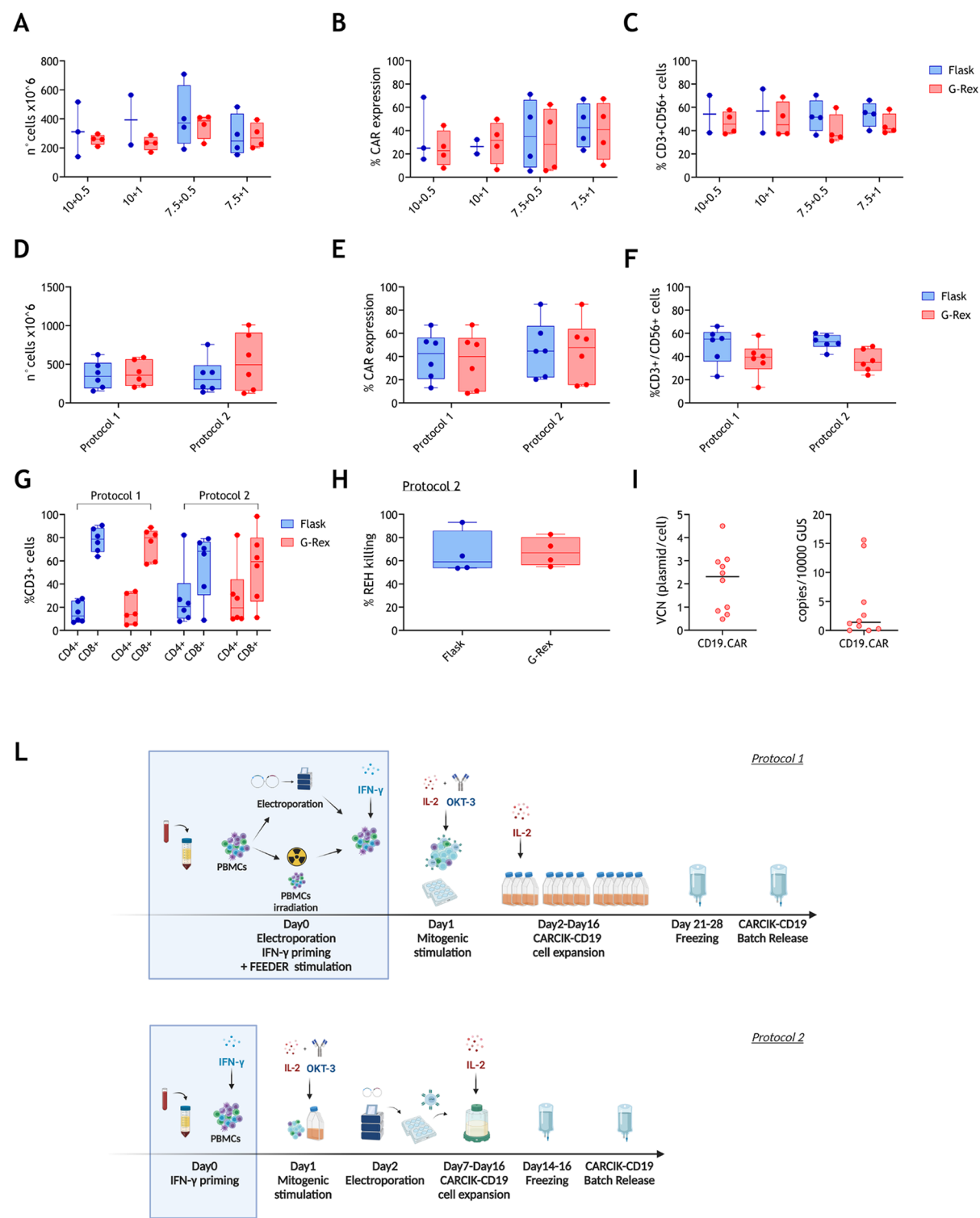


**Fig. 1** (See legend on next page.)

(See figure on previous page.)

**Fig. 1** Optimization of non-viral CARCIK cell platform. **(A–C)** CARCIK-CD19 cells were generated with titrated doses of pt4-CD19CAR and SB100X plasmids (in ug: 10+0.5; 10+1; 7.5+0.5; 7.5+1) and expanded in G-Rex or Flask. **(A)** Total cell yields at the end of the cell culture (starting from  $10 \times 10^6$  cells); **(B)** Percentage of CAR expression at the end of the differentiation gated on the CD3<sup>+</sup> subset; **(C)** Percentage of CD3<sup>+</sup>CD56<sup>+</sup> cells at the end of the differentiation. **(D–G)** CARCIK-CD19 cells were produced using either the standard Day 0 protocol (Protocol 1) or the feeder-free Day 2 protocol and expanded in G-Rex or Flasks (Protocol 2). **(D)** Total cell yields at the end of the cell culture (starting from  $10 \times 10^6$  cells); **(E)** Percentage of CAR expression; **(F)** Percentage of CD3<sup>+</sup>CD56<sup>+</sup> cells; **(G)** Percentage of CD4<sup>+</sup> and CD8<sup>+</sup> cells obtained between two different methods both in Flasks and G-Rex. **(H)** Short-term *in vitro* cytotoxicity of CARCIK-CD19 cells produced using the new Day 2 feeder-free protocol (in T-flasks and G-Rex) against the CD19<sup>+</sup> REH cell line, tested at an E:T ratio of 1:5. Results represent four independent experiments. **(I)** Vector copy number analysis (plasmid/cell) and transposase (copies/10000 GUS) gene expression by RT-PCR at the end of culture for CARCIK-CD19 cells produced with the Day 2 feeder-free protocol and expanded in G-Rex. **(L)** Schematic of the standard protocol in Flasks (Protocol 1) and optimized feeder free method in G-Rex (Protocol 2)

### G-Rex CARCIK-CD19 cells are transcriptionally different from flask-expanded products

The less differentiated immunometabolic and phenotypic characteristics of G-Rex-expanded CARCIK-CD19 cells were further validated at the transcriptional level. Gene expression analysis comparing CARCIK-CD19 cells produced in Flask or G-Rex confirmed significant transcriptional differences between the two products (Fig. 3A–B). Pathway score analysis confirmed that CARCIK cells cultured in the bioreactors displayed higher memory and lower glycolysis and glucose import scores. Additionally, the G-Rex culture method, which enhances oxygen access through nutrient convection [10, 13] resulted in a lower hypoxia score compared to Flask-expanded cells (Fig. 3C). Furthermore, G-Rex-expanded cells exhibited a less activated state, as indicated by lower cell cycle score and lower PI3K/AKT, NF-KB, and mTOR scores, lower scores of senescence/quiescence, exhaustion, and checkpoint signaling, with an increased chemokine signaling (Fig. 3C–D). Looking at the differentially regulated genes, we identified 24 genes, 11 upregulated and 13 downregulated in G-Rex vs. flask-expanded CARCIK-CD19 cells. Among the most upregulated was IL-10, which sustains mitochondrial fitness and promotes OXPHOS, leading to complete remission in multiple solid tumor models, as shown in a recent study on IL-10-secreting CAR T cells [22]. Furthermore, *SELL* gene was also upregulated, and this is known to correlate with a higher proportion of CM T cells<sup>10</sup> (Fig. 3F). By looking at the metabolic profile, we identified in the G-Rex group a downregulation of ALDOA, an enzyme crucial to glycolysis, further supporting that G-Rex culture skews CARCIK-CD19 cells towards a more oxidative metabolism. Overall, these findings on the transcriptional signatures suggest that the optimization made in the CARCIK production process led to improved cellular fitness.

### G-Rex expanded CARCIK-CD19 cells display a potent anti-tumor activity *in vivo*

In our previous work with CARCIK cells generated using Protocol 1, we established that the effective *in vivo* dose for tumor control was  $15 \times 10^6$  CAR<sup>+</sup> CIK cells [2]. Building on this, we investigated whether G-Rex-expanded

CARCIK cells (Protocol 2), with their distinct immunometabolic features, could achieve similar tumor control at reduced doses. To this end, DAUDI-engrafted mice were treated with escalating doses of  $5 \times 10^6$  (5 M),  $10 \times 10^6$  (10 M), and  $15 \times 10^6$  (15 M) CD19.CAR<sup>+</sup>CIK cells per mouse (Fig. 4A). While the 5 M dose was insufficient, the 10 M dose effectively controlled DAUDI cell growth. Mice treated with 10 M and 15 M doses exhibited comparable tumor control (Fig. 4B) and survival rates (Fig. 4C).

To validate these findings, two additional CARCIK-CD19 cell donors were tested *in vivo* using bioluminescence imaging (BLI). Daudi-FFLuc<sup>+</sup>-injected NSG mice received the same treatment regimen as in the initial experiment (Fig. 4D). At the 15 M dose, toxicity was observed in 4 out of 7 mice, attributed to a massive expansion of CD3<sup>+</sup> cells in the absence of disease (data not shown). This highlighted the superior efficacy-safety balance at the 10 M dose (Fig. 4E–G). Using RNAScope *in situ* hybridization, we detected CD19.CAR<sup>+</sup>CIK cells that were still present and infiltrated in the spleens of treated mice at sacrifice for both the 10 M and 15 M doses (Fig. 4H, Supplemental Fig. 2). These *in vivo* functional data demonstrate that lower doses of G-Rex-expanded CARCIK cells retain therapeutic efficacy while minimizing safety risks, supporting their consideration for future clinical applications.

### GMP validation of the streamlined production process of CARCIK-CD19 cells

The new CARCIK-CD19 cell expansion process was successfully validated under GMP conditions and the results are presented in Table 1. A total of seven batches were produced across our two cell manufacturing facilities: Lanzani Laboratory ( $n=4$ ) and Stefano Verri Laboratory ( $n=3$ ). All expansions were successful and allowed the production of clinically relevant numbers of cells. Cell viability exceeded 90%, and all quality- and safety-related product attributes (Table 1), including endotoxin levels, sterility, and mycoplasma (data not shown), met the required specifications. The consistency of this production process was further confirmed by the comparable results obtained from the two cell manufacturing facilities.

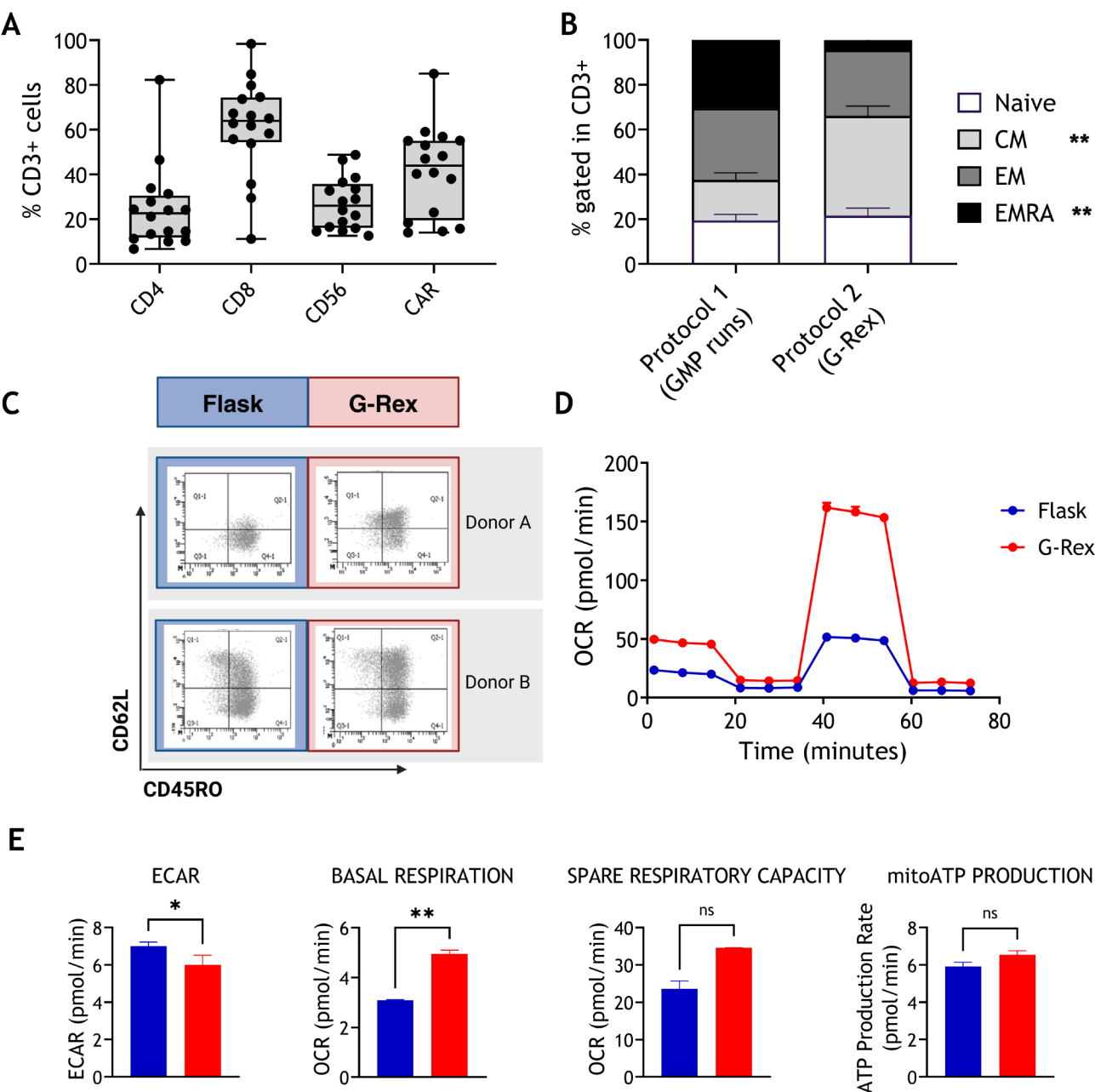


**Fig. 2** Differentiation and metabolic profiles of CARCIK cells. **(A)** Immunophenotype along with CAR expression of CARCIK-CD19 cells produced following Protocol 2. **(B)** Memory phenotype comparison between Protocol 1- and Protocol 2- derived CARCIK-CD19 cells. **(C–E)** Intradonor memory and metabolic differences (analyzed by Seahorse T Cell Metabolic Kit) between Flask- and G-Rex-derived CARCIK-CD19 cells generated following Protocol 2. OCR: Oxygen Consumption Rate ECAR: Extracellular Acidification Rate

We conclude that this streamlined approach simplified the overall process, allowing for consistent large-scale production, while maintaining high-quality standards.

Discussion

The genetic modification of T cells for CAR expression has been traditionally dominated by viral vector methods, which, despite their effectiveness, are encumbered by high costs, safety issues, and complex production

protocols. In the last decade, our research has aimed to address these challenges by exploring non-viral methods, specifically the Sleeping Beauty (SB) transposon system, which offers a safer and more economical alternative. Our previous work established the feasibility and safety of the SB system for engineering CAR T cells targeting various antigens, including CD19, in particular using CIK cells as effectors [2, 3, 23]. The clinical validation of CARCIK-CD19 cells in patients with relapsed B-Acute



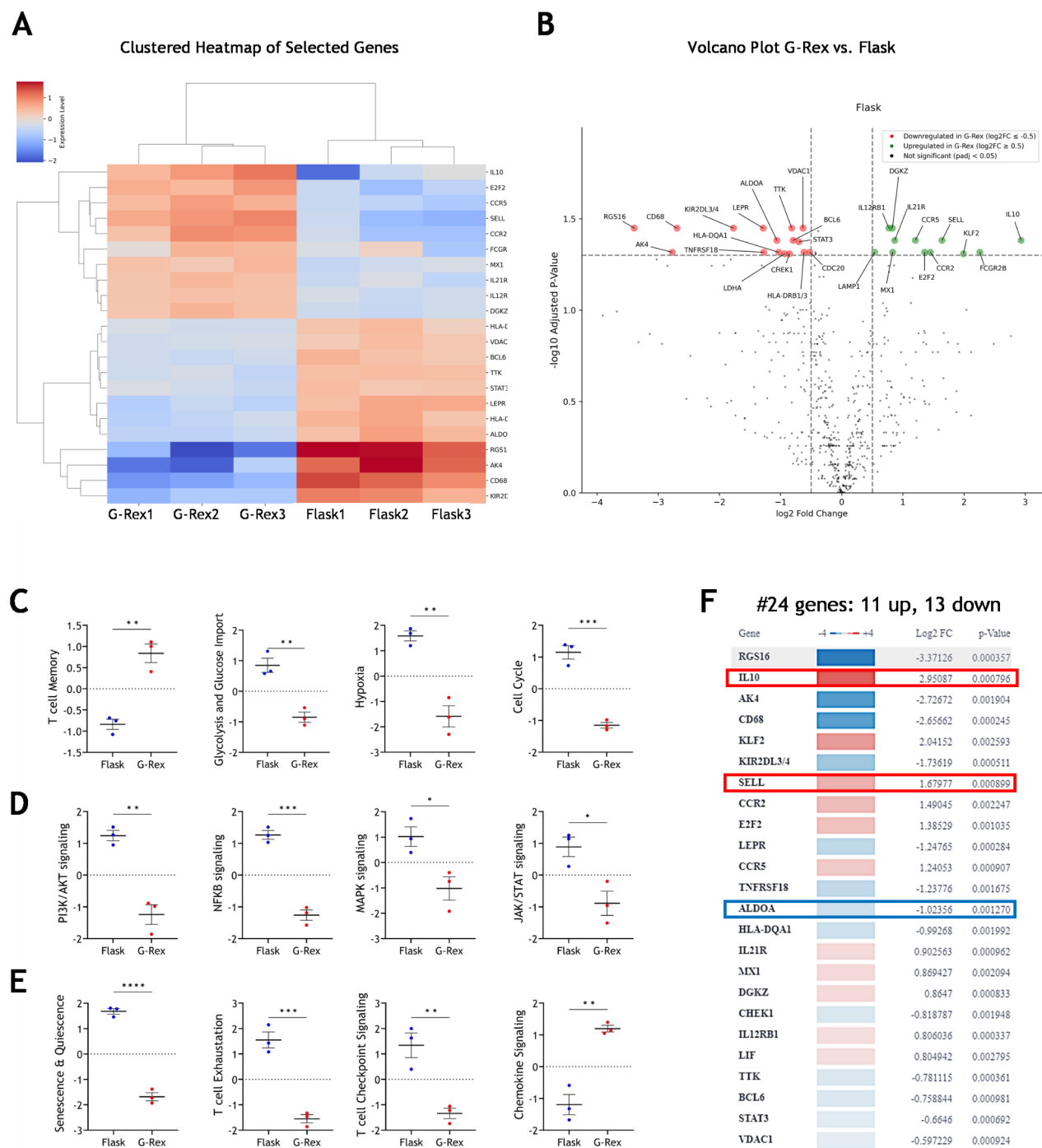


**Fig. 3** Gene expression characterization of Flask- and G-Rex derived CARCIK-CD19 cells. **(A)** Hierarchical clustering heatmap of Flask- and G-Rex- derived CARCIK-CD19 cells produced following Protocol 2. **(B)** Volcano plot of the differential gene expression analysis of Flask- and G-Rex- derived CARCIK-CD19. **(C–E)** Pathway analysis and **(F)** number of DEGs significantly up- and downregulated comparing Flask- and G-Rex- derived CARCIK-CD19 cells

Lymphoblastic Leukemia (ALL) demonstrated the potential of non-viral approaches in overcoming some limitations of viral vectors [6]. Our current study aimed to optimize the CARCIK-CD19 manufacturing process to enhance cell product quality and streamline production. Key improvements included reducing plasmid quantities to minimize nucleofection-related toxicity, eliminating the need for feeder PBMCs by postponing nucleofection from day 0 to day 2, and replacing T-flasks with the G-Rex bioreactor for cell expansion. The G-Rex system enabled a more efficient culture process by allowing for the addition of a larger volume of medium from the start

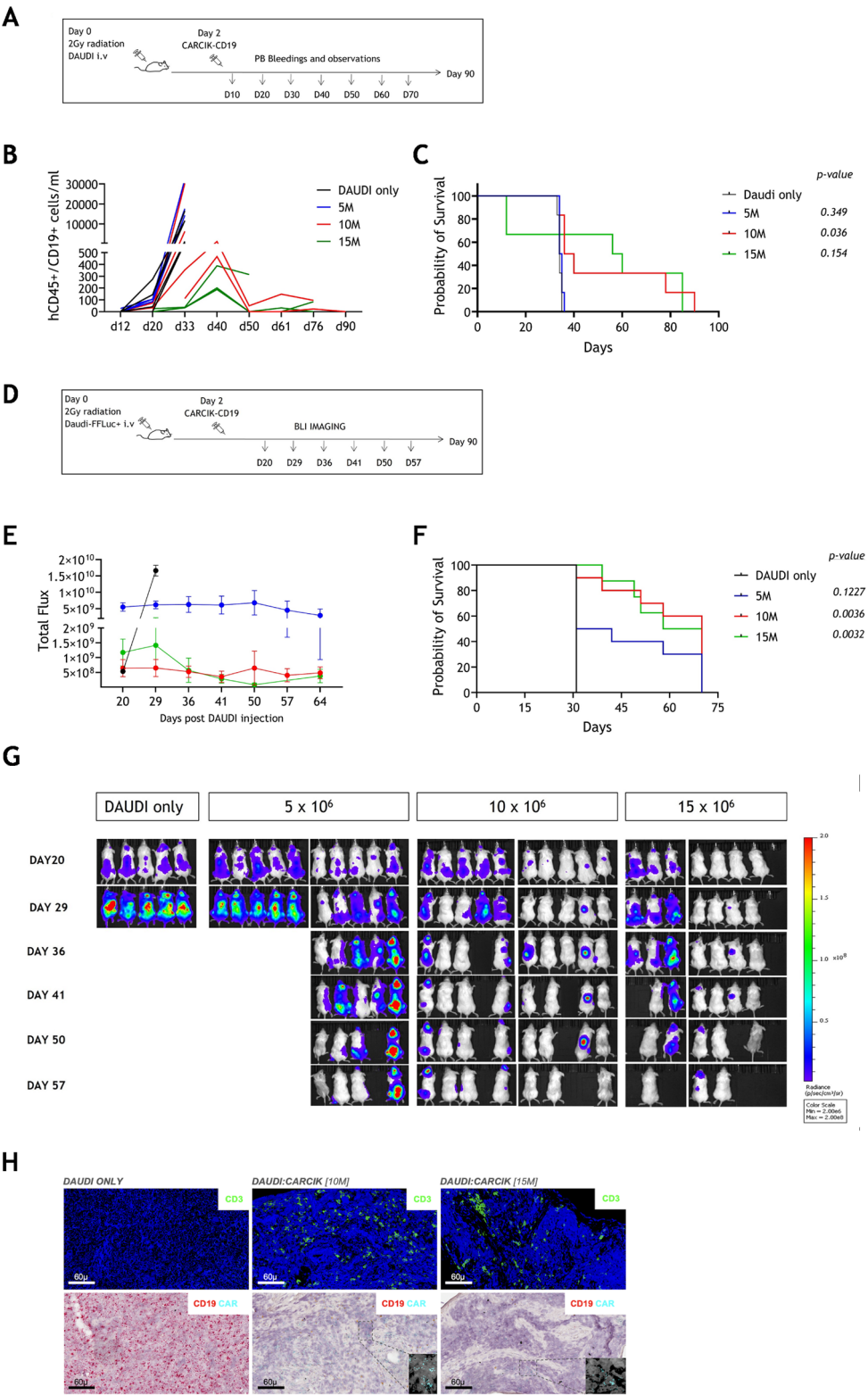


**Fig. 4** (See legend on next page.)

(See figure on previous page.)

**Fig. 4** Dose finding study of G-Rex derived CARCIK-CD19 cells (Protocol 2) in a survival DAUDI mouse model. **(A)** DAUDI-engrafted NSG mice model scheme. Mice were sub-lethally irradiated (2 Gy) and  $0.5 \times 10^6$  DAUDI cells were injected i.v. on Day 0. Mice were treated with  $5 \times 10^6$  (5 M),  $10 \times 10^6$  (10 M), and  $15 \times 10^6$  (15 M), CARCIK-CD19 cells at Day2 and bled every 10 days to quantify disease burden. **(B)** Analysis of hCD45<sup>+</sup>CD19<sup>+</sup> cells/ml in PB of untreated (DAUDI only) and treated (5 M, 10 M, and 15 M CARCIK-CD19 cells) mice. **(C)** Kaplan Meier survival curves of NSG mice engrafted with DAUDI cells, untreated or treated with CARCIK-CD19 cells. Comparisons of survival curves were determined by Log-rank test. **(D)** Scheme of DAUDI-FFLuc+ engrafted NSG mice. Mice were sub-lethally irradiated (2 Gy) and  $0.5 \times 10^6$  DAUDI-FFLuc+ cells were injected i.v. on Day0. Mice were treated with  $5 \times 10^6$  (5 M),  $10 \times 10^6$  (10 M), and  $15 \times 10^6$  (15 M), CARCIK-CD19 cells at Day2 and bioluminescence was performed weekly to follow the disease burden. **(E)** Tumor burden of DAUDI FFLuc+ cells in untreated and treated mice measured by bioluminescent imaging from day 20 after DAUDI injection. **(F)** Kaplan Meier survival curves of DAUDI engrafted NSG mice, left untreated or treated with CARCIK-CD19 cells. Comparisons of survival curves were determined by Log-rank test. **(G)** BLI imaging was performed using the IVIS lumina III imaging system. Tumor burden was visualized on days 20, 29, 36, 41, 50 and 57. **(H)** RNAscope in situ hybridization images showing CARCIK-CD19 and DAUDI cells in the spleen of untreated and treated (10 M and 15 M of CARCIK-CD19 cells) mice. Upper panels Representative pseudo-color fluorescence images showing automated staining for CD3 (green) on FFPE mouse spleen sections. The samples represent mice injected with DAUDI cells alone (left), DAUDI+CARCIK-CD19 cells (10 M, center), or DAUDI+CARCIK-CD19 cells (15 M, right). Representative Duplex RNAscope images of different FFPE slides of the same samples using probes targeting CAR (Channel 1, green dots) and CD19 (Channel 2, red dots). Images are shown at 40x magnification. Scale bars: 60  $\mu$ m

of culture, facilitating gas exchange and nutrient delivery, and avoiding repeated manipulation and splitting steps during culture. Indeed, culture in G-Rex implies only the addition of IL-2 during culture, without resuspension and counting, except at the end of culture, since the required quantity of medium is added only at the start [9, 13]. This approach not only shortened the culture period from 21 to 28 days to 14–17 days but also improved cell yield and quality. Although bioreactors entail an initial investment, the overall cost remains lower than that of flask-based methods due to the reduced consumption of culture medium, serum, and plasticware. Additionally, G-Rex considerably decreases the volume of medium required—by approximately 50% (data not shown)—further contributing to cost savings. The scalability and efficiency of G-Rex expansion streamline the manufacturing process, making it a more viable option for large-scale clinical applications. These economic and logistical advantages strongly support the choice of G-Rex expansion for our CARCIK cell manufacturing process. Moreover, an important advantage of G-Rex is the elimination of gamma-irradiated PBMCs, which, along with the reduced culture duration and minimal manual intervention, represents a significant advancement in simplifying and scaling up CARCIK cell production. These benefits collectively position the G-Rex system as a cost-effective and practical solution for the efficient generation of CARCIK cells, particularly in the context of clinical translation and large-scale manufacturing.

Our findings demonstrated that CARCIK-CD19 cells expanded in G-Rex bioreactors and exhibited a more favorable memory T cell profile compared to those cultured in flasks. Indeed, the G-Rex-expanded cells showed a higher proportion of CM and naïve T cells, which are associated with improved persistence and enhanced anti-tumor activity [18, 19]. This was corroborated by metabolic profiling, which revealed a shift towards mitochondrial respiration in G-Rex cells, indicative of a more robust and less differentiated phenotype. The transcriptional analysis further highlighted the advantages of the

new production process in G-Rex. CARCIK-CD19 cells from G-Rex exhibited distinct gene expression profiles, including upregulation of genes associated with mitochondrial function and downregulation of glycolytic pathways. This suggests that the G-Rex culture method supports a more oxidative metabolism and less activation-induced differentiation, contributing to improved cellular fitness.

*in vivo* studies reinforced the potential of G-Rex-expanded CARCIK-CD19 cells. The reduced cell dose required for effective tumor control in mouse models underlined the enhanced potency of these cells. The ability to achieve significant anti-tumor effects with fewer cells not only has implications for reducing treatment costs but also minimizes potential side effects associated with high cell doses.

The GMP validation of the streamlined production process confirmed its consistency and reproducibility across different manufacturing facilities. With the successful production of seven batches and high-quality metrics, including over 90% cell viability and compliance with endotoxin and sterility specifications, this optimized process meets the rigorous standards required for clinical applications.

Overall, the integration of the G-Rex bioreactor system with the SB transposon technology represents a significant advancement in CARCIK cell manufacturing. This streamlined approach enhances the efficiency, scalability, and cost-effectiveness of CARCIK-CD19 cell production, paving the way for broader clinical applications and potential improvements in patient outcomes. Finally, G-Rex devices are disposable containers that can be more easily implemented by academic GMP production facilities compared to more complex automated devices.

Indeed, building on these promising results, we have initiated a new clinical protocol to further evaluate the efficacy of the optimized CARCIK-CD19 cells. This phase I/II study will investigate the use of these cells in treating adult and pediatric patients with relapsed/refractory mature CD19<sup>+</sup> B-NHL and CLL. The new clinical trial

**Table 1** GMP validation of CARCIK-CD19 cell expansion

CARCIKCD19 Batch n°	TNC fold increase (from day +7)	Viability (%)	CD3 (%)	CD3+/CAR+ (%)	Vector Copy Number (copies/cell)	SB100X Transposase (copies/10000 GUS)	Cytotoxicity (%)
CARCIKCD19-BG28	101,64	96,7	98,7	14,6	0,98	1,55	60,9
CARCIKCD19-BG30	73,11	95,4	99,8	40,3	1,23	1,44	82,9
CARCIKCD19-BG35	121,33	90,8	98,4	55,1	0,85	0,57	72,7
CARCIKCD19-BG37	60,72	89,1	99,3	56,9	1,77	1,19	55,0
CONV-GREX01	37,78	97,7	99,4	36,1	1,30	18,26	89,2
CONV-GREX02	83,7	95,3	98,1	38,5	1,29	4,36	70,3
CONV-GREX03	91,07	92,1	96,7	55,2	3,29	19,97	91,0
Mean	81,34	93,9	98,6	42,4	1,5	6,8	74,6
Standard deviation	23,79	3,2	1,1	15,1	0,8	8,5	13,8
Specifications	n/a	≥ 80%	≥ 90%	≥ 10%	< 5	< 20	≥ 25%

(NCT05869279) will assess the impact of the enhanced CARCIK-CD19 cells on patient outcomes, including response rates and overall survival, further validating the clinical utility of our streamlined production process.

Conclusions

This study refines non-viral CARCIK-CD19 production using G-Rex bioreactors, streamlining manufacturing, enhancing cell fitness, and boosting therapeutic efficacy. The GMP-compliant, scalable protocol offers a safer, cost-effective alternative for treating relapsed/refractory CD19+ lymphomas, with significant clinical potential and broad scalability.

Abbreviations

allo-HSCT	Allogeneic hematopoietic stem cell transplantation
AML	Acute myeloid leukemia
ATMPs	Advanced therapy medicinal products
B-ALL B-cell	Acute lymphoblastic leukemia
B-NHL B-cell	Non-hodgkin lymphoma
CAR	Chimeric Antigen Receptor
CIK	Cytokine-induced killer
CLL	Chronic lymphocytic leukemia
ECAR	Extracellular acidification rate
FBS	Fetal bovine serum
FFLuc	Firefly luciferase
FFPE	Formalin-fixed, paraffin-embedded
GMP	Good manufacturing practice
G-Rex	Gas-permeable rapid expansion
GUS	β-glucuronidase gene
IR	Inverted repeat

IVIS	<i>in vivo</i> imaging system
MNDU3	Synthetic MNDU3 promoter
MNCs	Mononuclear cells
NSG	NOD scid gamma mouse model
OCR	Oxygen consumption rate
PPIB	Peptidyl-prolyl cis-trans isomerase B
TILs	Tumor-infiltrating lymphocytes
Tregs	Regulatory T cells
VCN	Vector copy number

Supplementary information

The online version contains supplementary material available at <https://doi.org/10.1186/s12967-025-06416-3>.

Supplementary Material 1

Acknowledgements

The authors would like to thank the parent committees Quelli che...con LUCA Onlus, Comitato Maria Letizia Verga, Fondazione Pino Camerani ed Elisabetta Pintaldi, Associazione Italiana Lotta alla Leucemia, Linfoma e Mieloma (AIL) sezione Paolo Belli Bergamo, Amici di Duccio, and Stefano Verri for their generous and constant support and Benecyte, Inc. for providing the SB plasmids.

Authors’ contributions

I.Pisani: data curation, formal analysis, validation, investigation, visualization, methodology. G.Melita: data curation, formal analysis, validation, investigation, visualization, methodology, review and editing. P.B. De Souza: data curation, validation, formal analysis. S. Galimberti: data curation formal statistical analysis and methodology. A.M.Savino: data curation, validation, formal analysis. J.Sarno: validation, formal analysis. B.Landoni: data curation, validation, formal analysis. S.Crippa: data curation, investigation, methodology. E.Gotti: data curation, validation, formal analysis, investigation, methodology, review and

editing. C.Cuofano: data curation, validation, formal analysis, investigation, methodology. O. Pedrini: validation, formal analysis, methodology. C.Capelli: validation, formal analysis, methodology. G.Matera: data curation, validation, formal analysis, methodology. D.Belotti: data curation, validation, methodology. S.Cesana: validation, formal analysis. B.Cabati: validation, formal analysis, methodology. M.Quaroni: data curation, validation, formal analysis, methodology. V.Colombo: validation, formal analysis, methodology. M.Mazza: formal analysis, methodology, writing, review and editing. B.Vergani: data curation, validation, methodology. A.Gaimari: formal analysis, methodology. F.Nicolini: data curation, formal analysis, methodology. M.Tazzari: data curation, formal analysis, validation, methodology, writing-review and editing. M.Bocchini: data curation, formal analysis, validation, methodology. M.Serafini: review and editing. A.Rambaldi: conceptualization, resources, supervision, funding acquisition, review and editing. B.Rambaldi: conceptualization, writing-review and editing. G.Dastoli: conceptualization, review and editing. A.Biondi: conceptualization, resources, supervision, funding acquisition, review and editing. G.Gaipa: conceptualization, resources, supervision, funding acquisition, writing-review and editing. M.Introna: conceptualization, resources, supervision, funding acquisition, writing-review and editing. J.Golay: conceptualization, supervision, writing-review and editing. S.Tettamanti: conceptualization, data curation, formal analysis, validation, investigation, visualization, methodology, funding acquisition, writing-review and editing.

### Funding

The work was supported by grants AIRC 5 × 1000 “Immunity in Cancer Spreading and Metastasis (ISM)” (grant 21147), AIRC MFAG 2024 ID 30974; Fondazione Regionale per la Ricerca Biomedica (FRRB, Regione Lombardia), Project N°CP2\_10/2018 “Plagencell”, Italian PNRR CN3 “National Center for Gene Therapy and Drugs based on RNA Technology” and LSH-TA Ecosistema innovativo della Salute. The authors were also supported by the Italian Ministry of Health through the “Research Project on CAR-T cells for hematological malignancies and solid tumors”, as part of the Alliance Against Cancer (ACC) network initiative.

### Data availability

The datasets used and/or analyzed during the current study are available from the corresponding author on reasonable request.

### Declarations

#### Ethics approval and consent to participate

The *in vivo* studies were approved by the Italian Ministry of Health. Procedures involving animals were conformed with protocols approved by the Milano-Bicocca University in compliance with national and international law and policies. All *in vivo* experiments were conducted at the University of Milano-Bicocca.

#### Consent for publication

Not applicable.

#### Competing interests

The authors declare that they have no competing interests.

#### Author details

<sup>1</sup>Tettamanti Center, Fondazione IRCCS San Gerardo dei Tintori, Monza, Italy

<sup>2</sup>Advanced Cellular Therapies and Rare Tumors Unit, IRCCS Istituto Romagnolo per lo Studio dei Tumori (IRST) “Dino Amadori” S.r.l., Meldola, Italy

<sup>3</sup>Bicocca Bioinformatics Biostatistics and Bioimaging B4 Center, School of Medicine and Surgery, University of Milano-Bicocca, Monza, Italy

<sup>4</sup>Department of Medicine and Surgery, University of Milano-Bicocca, Milan, Italy

<sup>5</sup>Center of Cellular Therapy “G. Lanzani”, Division of Hematology, ASST Papa Giovanni XXIII, Bergamo 24122, Italy

<sup>6</sup>Laboratorio di Terapia Cellulare e Genica Stefano Verri, Fondazione IRCCS San Gerardo dei Tintori, Monza, Italy

<sup>7</sup>Department of Oncology and Hematology, University of Milan, Milan, Italy

<sup>8</sup>Department of Oncology-Hematology, Azienda Socio-Sanitaria Territoriale Papa Giovanni XXIII, Bergamo, Italy

Received: 18 January 2025 / Accepted: 25 March 2025

Published online: 19 May 2025

### References

1. Magnani CF, Tettamanti S, Alberti G, Pisani I, Biondi A, Serafini M et al. Transposon-Based CAR T Cells in Acute Leukemias: Where are We Going? *Cells*. 2020 May 27 [cited 2021 Dec 13];9(6). Available from: <https://pubmed.ncbi.nlm.nih.gov/32471151/>
2. Magnani CF, Mezzanotte C, Cappuzzello C, Bardini M, Tettamanti S, Fazio G et al. Preclinical efficacy and safety of CD19CAR Cytokine-Induced killer cells transfected with sleeping beauty transposon for the treatment of acute lymphoblastic leukemia. *Hum Gene Ther*. 2018;29(5).
3. Rotiroti MC, Buracchi C, Arcangeli S, Galimberti S, Valsecchi MG, Perriello VM et al. Targeting CD33 in Chemoresistant AML Patient-Derived Xenografts by CAR-CK Cells Modified with an Improved SB Transposon System. *Mol Ther*. 2020 Sep 2 [cited 2021 Apr 1];28(9):1974–86. Available from: <https://pubmed.ncbi.nlm.nih.gov/32526203/>
4. Perriello VM, Rotiroti MC, Pisani I, Galimberti S, Alberti G, Pianigiani G, et al. IL-3-zetakine combined with a CD33 costimulatory receptor as a dual CAR approach for safer and selective targeting of AML. *Blood Adv*. 2023;7(12):2855–71.
5. Turazzi N, Fazio G, Rossi V, Rolink A, Cazzaniga G, Biondi A et al. Engineered T cells towards TNFRSF13C (BAFFR): a novel strategy to efficiently target B-cell acute lymphoblastic leukaemia. Vol. 182, *British journal of haematology*. England; 2018. pp. 939–43.
6. Magnani CF, Gaipa G, Lussana F, Belotti D, Gritti G, Napolitano S, et al. Sleeping Beauty-engineered CAR T cells achieve antileukemic activity without severe toxicities. *J Clin Invest*. 2020;130(11):6021–33.
7. Watanabe N, Mo F, McKenna MK. Impact of manufacturing procedures on CAR T cell functionality. *Front Immunol*. 2022;13:876339.
8. Gotti E, Tettamanti S, Zaninelli S, Cuofano C, Cattaneo I, Rotiroti MC, et al. Optimization of therapeutic T cell expansion in G-Rex device and applicability to large-scale production for clinical use. *Cytotherapy*. 2022;24(3):334–43.
9. Bajgain P, Mucharla R, Wilson J, Welch D, Anurathapan U, Liang B, et al. Optimizing the production of suspension cells using the G-Rex M series. *Mol Ther Methods Clin Dev*. 2014;1:14015.
10. Forget M-A, Haymaker C, Dennison JB, Toth C, Maiti S, Fulbright OJ, et al. The beneficial effects of a gas-permeable flask for expansion of Tumor-Infiltrating lymphocytes as reflected in their mitochondrial function and respiration capacity. *Oncoimmunology*. 2016;5(2):e1057386.
11. Chakraborty R, Mahendravada A, Perna SK, Rooney CM, Heslop HE, Vera JF, et al. Robust and cost effective expansion of human regulatory T cells highly functional in a xenograft model of graft-versus-host disease. *Haematologica*. 2013;98(4):533–7.
12. Xiao L, Chen C, Li Z, Zhu S, Tay JC, Zhang X, et al. Large-scale expansion of Vγ9Vδ2 T cells with engineered K562 feeder cells in G-Rex vessels and their use as chimeric antigen receptor-modified effector cells. *Cytotherapy*. 2018;20(3):420–35.
13. Ludwig J, Hirschel M. Methods and process optimization for Large-Scale CAR T expansion using the G-Rex cell culture platform. *Methods Mol Biol*. 2020;2086:165–77.
14. Challita PM, Skelton D, el-Khoueiry A, Yu XJ, Weinberg K, Kohn DB. Multiple modifications in Cis elements of the long terminal repeat of retroviral vectors lead to increased expression and decreased DNA methylation in embryonic carcinoma cells. *J Virol*. 1995;69(2):748–55.
15. Ivics Z, Hackett PB, Plasterk RH, Izsvák Z. Molecular reconstruction of sleeping beauty, a Tc1-like transposon from fish, and its transposition in human cells. *Cell*. 1997;91(4):501–10.
16. Mátés L, Chuah MKL, Belay E, Jerchow B, Manoj N, Acosta-Sanchez A, et al. Molecular evolution of a novel hyperactive sleeping beauty transposase enables robust stable gene transfer in vertebrates. *Nat Genet*. 2009;41(6):753–61.
17. CF M, G G, F L, D B, G G, S N, Sleeping Beauty-engineered CAR T cells achieve antileukemic activity without severe toxicities. *J Clin Invest*. 2020 Nov 2 [cited 2021 Sep 15];130(11):6021–33. Available from: <https://pubmed.ncbi.nlm.nih.gov/32780725/>
18. Deng Q, Han G, Puebla-Osorio N, Ma MCJ, Strati P, Chasen B et al. Characteristics of anti-CD19 CAR T cell infusion products associated with efficacy and toxicity in patients with large B cell lymphomas. *Nat Med*. 2020 Dec 1 [cited



- 2022 Aug 6];26(12):1878–87. Available from: <https://pubmed.ncbi.nlm.nih.gov/33020644/>
19. Fraietta JA, Lacey SF, Orlando EJ, Pruteanu-Malinici I, Gohil M, Lundh S et al. Determinants of response and resistance to CD19 chimeric antigen receptor (CAR) T cell therapy of chronic lymphocytic leukemia. *Nat Med*. 2018 May 1 [cited 2022 Aug 6];24(5):563–71. Available from: <https://pubmed.ncbi.nlm.nih.gov/29713085/>
  20. van der Windt GJW, Everts B, Chang C-H, Curtis JD, Freitas TC, Amiel E, et al. Mitochondrial respiratory capacity is a critical regulator of CD8 + T cell memory development. *Immunity*. 2012;36(1):68–78.
  21. Pearce EL, Pearce EJ. Metabolic pathways in immune cell activation and quiescence. *Immunity*. 2013;38(4):633–43.
  22. Zhao Y, Chen J, Andreatta M, Feng B, Xie Y-Q, Wenes M et al. IL-10-expressing CAR T cells resist dysfunction and mediate durable clearance of solid tumors and metastases. *Nat Biotechnol*. 2024 Nov;42(11):1693–1704
  23. Magnani CF, Turazzi N, Benedicenti F, Calabria A, Tenderini E, Tettamanti S, et al. Immunotherapy of acute leukemia by chimeric antigen receptor-modified lymphocytes using an improved *Sleeping Beauty* transposon platform. *Oncotarget*. 2014; Available from: <http://www.oncotarget.com/abstract/9955>.

### Publisher's note

Springer Nature remains neutral with regard to jurisdictional claims in published maps and institutional affiliations.